RSC Advances

ROYAL SOCIETY OF CHEMISTRY

www.rsc.org/advances

Journal Name

ARTICLE

Preparation of $Ni(OH)_2$ Nanosheets on Ni Foam Via Direct Precipitation Method for Highly Sensitive Non-enzymatic Glucose Sensor

Received 00th April 20xx,
Accepted 00th April 20xx

DOI: 10.1039/x0xx00000x

www.rsc.org/

Yudong Zhao[a], Gaochen Gu[b], Shengquan You[a], Renhua Ji[c], Hui Suo†[a], Chun Zhao†[a] and Fengmin Liu[a]

$Ni(OH)_2$ nanosheets on Ni foam was prepared by the direct precipitation method. The morphology and phase composition of the as-prepared $Ni(OH)_2$ nanosheets/Ni electrode were characterized by scanning electron microscopy and X-ray diffraction, respectively. The electrode's electrochemical behavior was investigated by cyclic voltammetry and the constant potential amperometry technique. The best performance of the glucose sensor can be obtained at 0.51 V in 0.2 M sodium hydroxide solution. The as-prepared $Ni(OH)_2$ nanosheets/Ni electrode shows high sensitivity with 1130 μAmM-1cm^{-2} at the glucose concentration range of 2 μM to 40 μM and 1097 μAmM^{-1}cm^{-2} at the range of 0.1 mM to 2.5 mM. The response time of this electrode is less than 2 seconds, and its detection limit is 1 μM.

1. Introduction

Glucose biosensors are widely used in the field of food industry, clinic diagnostics, and biochemical analysis [1, 2]. Efficient, fast and reliable measurement of glucose is greatly needed, especially in clinical diagnostics[3]. Therefore, much effort has been put into the development of electrocatalytic glucose sensors[4-6]. Glucose oxidase based biosensors have demonstrated some useful applications. However, these enzyme type sensors suffer from the insufficient stability of enzyme activity during the immobilization process and even in the storage period, which cause a significant problem to most sensor designs [7]. As an attractive alternative to overcome some of the limitations of enzymatic biosensors, non-enzymatic sensors have received increasing interest in recent years.

Various noble metals (e.g. Pt, Au, Ni and Cu), alloys (e.g. Pt-Pb), and oxides (e.g. NiO, $Ni(OH)_2$ and CuO) have been investigated in the development of effective non-enzymatic glucose sensors[8]. Compared with noble metals, copper and nickel oxide have been attracted more attention because of their lower cost and more excellent catalytic performance for nonenzymatic glucose sensing in alkaline medium[9-11]. The electrochemical oxidation of glucose by the $Ni(OH)_2$/NiOOH redox couple formed on the electrode surface in alkaline medium makes nickel of particular interest[12-16].

Ni-based glucose electrochemical biosensors have been fabricated on the capillary electrode such as a nanopore polycarbonate membrane template [16]or a Ti/TiO_2 nanotube array[17]. However, these methods suffer from complex and time-consuming synthesis routes. It is therefore expected the direct use of Ni foil is more convenient and applicable to he glucose sensor chip, but the sensitivity of this sensor only achieved 670 μA/mM-cm^2[18]. Ni foam has been drawn attentions due to its advantages such as high conductivity, three dimensional network structure and much higher loading amount of active materials per unit electrode area[19-21].

Nanostructure materials possess large surface-to-volume ratio and high active sites, thus favoring a greater and faster reaction between the glucose solution and the electrode. It is well known the electrochemical performance of the nickel nanostructure electrode may be regulated by the control of many factors such as particle size, surface morphology, composition and structure. Therefore, the controlled synthesis of novel metal oxide nanostructures is of considerable interest to achieve the required size, morphology and structure of the nanostructure. To the best of our knowledge, there are very few reports on the $Ni(OH)_2$ nanosheets on Ni foam prepared by the direct precipitation method for the non-enzymatic glucose sensing applications.

In this work, $Ni(OH)_2$ nanosheets on Ni foam was prepared by the direct precipitation method. This preparation method is simple, low temperature and cost effective synthesis method in the preparation of $Ni(OH)_2$ nanostructure on Ni foam for the non-enzymatic glucose sensor applications.

[a] State Key Laboratory on Integrated Optoelectronics, College of Electronic Science and Engineering, Jilin University, Changchun, Jilin Province, 130012, P.R.China
[b] Key Laboratory for the Physics and Chemistry of Nanodevices, Department of Electronics, Pekin University, Beijing 100871, P.R. China.
[c] Key Laboratory for the Physics and Chemistry of Nanodevices Department of Electronics, Peking University, Beijing 100871 P. R. China

† Corresponding author. Tel.: 86 13944911205; fax: 86 0431-85168242-8440 .
E-mail address: suohui@jlu.edu.cn (H. Suo); zhaochun@jlu.edu.cn(C. Zhao).

2. Experimental details

2.1 Reagents and apparatus

All Chemicals including nickel nitrate ($Ni(NO_3)_2$), aqueous ammonia analytically pure ($NH_3 \bullet H_2O$), glucose ($C_6H_{12}O_6$), sodium hydroxide (NaOH), ethanol (C_2H_6O), hydrochloric acid (HCl), were of analytical grade and used as received without further purification.

The electrode surface morphology was observed by an environmental scanning electron microscopy (XL30 FEG ESEM, FEI Company, United States), whereas the crystalline phase was examined by an X-ray diffraction (XRD) system with Cu Kα radiation (λ = 0.15405 nm) (Rigaku Company, Japan).

2.2 Preparation of the $Ni(OH)_2$/Ni electrode

A nickel foam plate with a thickness of 0.1 mm was sheared into an approximately 1.0 cm × 1.0 cm, which was then used as the electrode substrate. The nickel plate was polished by abrasive paper and washed with dilute hydrochloric acid and acetone in the ultrasonic cleaners for approximately 3 minutes to clear up the surface impurities. Deionized water was then used to wash up the residual reagents. Subsequently, the samples were placed into a plastic tube containing 4 mL 0.1 M $Ni(NO_3)_2$ and different volumes (10, 30 and 50 μL) of pure aqueous ammonia ($NH_3 \bullet H_2O$). The plastic tube was then placed into the Constant Temperature Incubator. The temperature was kept at 30 °C for an appropriate time (8, 10 and 16 hours). The samples were then removed, rinsed with deionized water, and dried at 40 °C.

2.3 Characterizations

Electrochemical experiments were performed using an electrochemical workstation (CHI660D, Chenhua Instruments Company of Texas, USA). This electrochemical cell consists of a three-electrode system with a $Ni(OH)_2$/Ni electrode (1.0 cm×1.0 cm) as the working electrode, an Ag/AgCl electrode was used as the reference electrode and a platinum as the counter electrode. Cyclic voltammetry (CV) was performed in a 0.2 M sodium hydroxide solution with a potential range of 0 to 0.7 V at the scan rate of 50 mVs-1 to observe the redox peaks and detect the stability. The electrode evaluation was performed by the constant potential amperometric technique in a 0.2 M sodium hydroxide solution with continuous stirring. Approximately 5 μL of the 0.2 M glucose solution was injected at regular intervals so that the resultant concentration varied from 10 μM to 3 mM. All the experiments were conducted at the environment temperature (25 °C).

3. Results and discussion

3.1 Characterization of the $Ni(OH)_2$/Ni electrode

The morphologies and microstructures of the obtained $Ni(OH)_2$/Ni electrodes were characterized by field emission SEM. As shown in Fig. 1, the $Ni(OH)_2$ nanosheets evenly and compactly covered the surface of the Ni foam. The nickel nitrate probably reacted continually with aqueous ammonia to form the monodisperse nickel hydroxide particles. Subsequently, these monodisperse particles agglomerated with each other to form the nanosheets on the nickel foam surface.

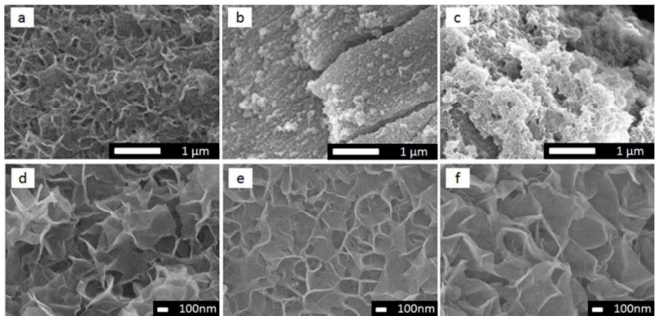

Fig. 1 SEM images (a–d) of $Ni(OH)_2$/Ni electrodes prepared with 4 mL 0.1 M $Ni(NO_3)_2$ and 10 (a), 30 (b), and 50 μL (c) analytically pure aqueous ammonia at 30 °C for 8 (d), 10 (e), and 16 hours (f), respectively.

From Figs. 1a to 1c, the increasing volume of aqueous ammonia in the reaction solution results in the high aggregation and non-uniformity of nanoparticles and nanosheets on the Ni substrate, so the 10 μL aqueous ammonia is enough to prepare the $Ni(OH)_2$/Ni electrodes. The reaction time also affects the growth of the $Ni(OH)_2$/Ni electrodes, which are shown in Figs. 1d to 1f. The uniform the compact films composed of nanosheets can be achieved under the depositing time of 10 hours. Thus, we further investigated the performance of the $Ni(OH)_2$ nanosheets /Ni electrodes grown in the 10 μL aqueous ammonia and deposited for 10 hours.

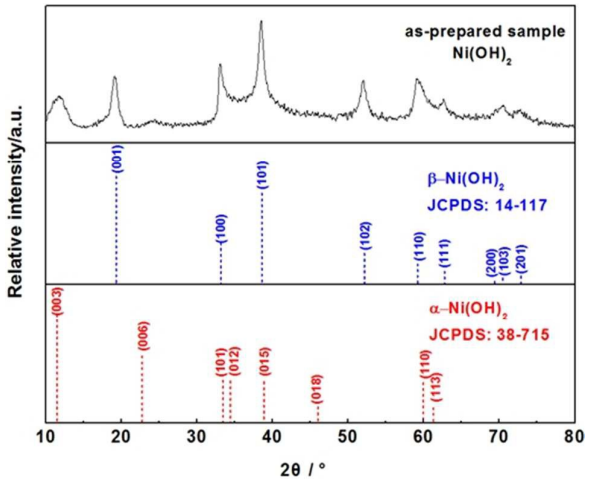

Fig. 2 XRD patterns of the as-prepared $Ni(OH)_2$/Ni material prepared with 4 mL 0.1 M $Ni(NO_3)_2$ and 10 μL analytically pure aqueous ammonia at 30 °C for 10 hours.

The XRD patterns of the as-prepared $Ni(OH)_2$ nanosheets films are shown in Fig. 2, which exhibits several well-defined

diffraction peaks. According to the JCPDS cards of no. 14-0117/38-0715, the diffraction peaks of 2θ = 11.01°, 21.97°, 33.7°, 60.43° show the typical characteristics of α-$Ni(OH)_2$. Similarly, the diffraction peaks of 2θ = 19.34°, 33.1°, 38.6°, 52.12°, 59.1°, 62.7°, 70.7° show the typical characteristics of β-$Ni(OH)_2$. These values indicate that the $Ni(OH)_2$ nanoparticles deposited on the nickel foam are the mixture of α-$Ni(OH)_2$ and β-$Ni(OH)_2$ [22, 23].

3.2 Electrochemical performance of the $Ni(OH)_2$ nanosheets / Ni electrodes

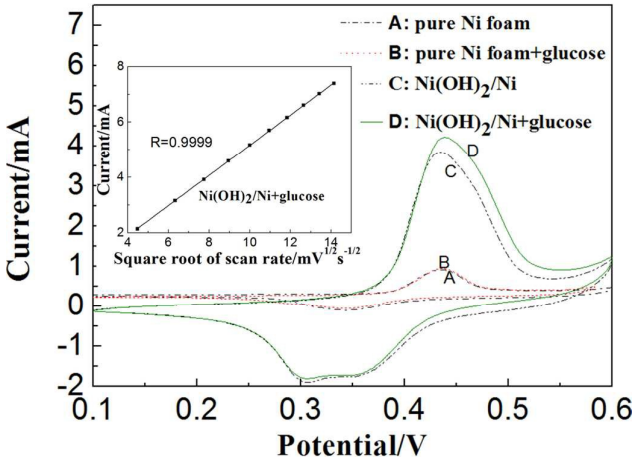

Fig. 3 CVs of the Ni foam and the as-prepared $Ni(OH)_2$/Ni electrode with and without glucose (0.2 mM) in 0.2 M NaOH solution. The inset is oxidation peak currents to the potential scan rate of the as-prepared $Ni(OH)_2$/Ni electrode with glucose. The scan rate is 50 mVs^{-1}.

The Ni foam and $Ni(OH)_2$ nanosheets /Ni electrode were tested in 0.2 M sodium hydroxide solution with and without glucose by CV to examine the electrochemical characterization of the as-prepared $Ni(OH)_2$ nanosheets /Ni electrode. The resultant cyclic voltammograms were shown in Fig. 3. Curve A and B in Fig.3 is the cyclic voltammogram of the bare Ni foam in the sodium hydroxide solution without and with glucose, respectively. The current value of oxidation peak in Curve A was less than 1mA and increased a little at the presence of glucose (curve B), indicating that the bare Ni foam electrode has poor catalytic performance. Curve C and D in Fig.3 is the cyclic voltammogram of the $Ni(OH)_2$ nanosheets /Ni electrode in the sodium hydroxide solution without and with glucose, respectively. A pair of well-defined oxidation and reduction peaks can be clearly observed. This is ascribed to the redox reaction of $Ni(OH)_2$/NiOOH, indicating that the electrochemical process was semi-reversible [24]. The current value of the oxidation peak slightly increased in the presence of glucose (0.2 mM) in the sodium hydroxide solution (curve D). As shown in curve D, one oxidation peak at +0.44 V and two reduction peaks at +0.30 V and +0.37 V are observed. As discussed in Fig.2, two kinds of $Ni(OH)_2$ with different crystal phases exist on the surface of the Ni foam. According to ref.[23], the reduction peak potentials of β-$Ni(OH)_2$ are higher than that of α-$Ni(OH)_2$, whereas the migration rate of protons in β-$Ni(OH)_2$ is much smaller than that in α-$Ni(OH)_2$. Thus, the reduction peak at +0.37 V is ascribed to β-$Ni(OH)_2$, whereas the reduction peak at +0.30 V is ascribed to α-$Ni(OH)_2$.

The redox peak current increases with the potential scan rate, which was shown in the inset of Fig.3. The redox peak currents are proportional to the square root of the scan rates with the correlation coefficient values of 0.9999, indicating that this reaction is controlled by the diffusion process of OH^- [25].

3.3 Electrocatalytic oxidation of glucose

3. 3. 1 Electrocatalytic oxidation mechanism of glucose

The CV of the as-prepared $Ni(OH)_2$ nanosheets/Ni electrode was performed in 0.2 M sodium hydroxide solution with different glucose concentration from 0.3 mM to 1.8 mM at a scan rate of 50 mVs^{-1} to further examine the oxidation mechanism of the as-prepared $Ni(OH)_2$ nanosheets/Ni electrode for glucose. Fig.4 shows the resultant cyclic voltammograms. The in-set of Fig.4 shows the linear relationship between the oxidation peak current values and corresponding glucose concentration.

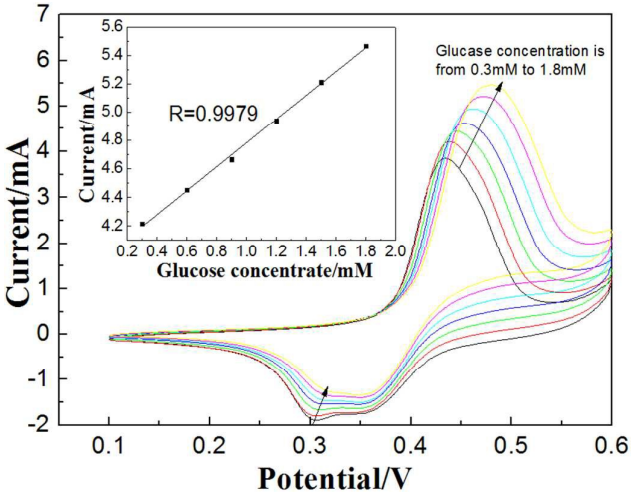

Fig. 4 CVs of the $Ni(OH)_2$/Ni electrode in 0.2 M NaOH solution containing different glucose concentrations from 0.3 mM to 1.8 mM. The in-set is the corresponding calibration plot of the oxidation peak current to glucose concentration.

It can be seen from Fig.4 when the glucose solution was added into the electrolytic cell, the oxidation peak current clearly increased, whereas the reduction peak current slightly decreased. As CV was performed, $Ni(OH)_2$ was transformed into NiOOH at the oxidation peak. The ionization energy of Ni^{+3} is 3393 $kJmol^{-1}$, which results in a strong oxidation capacity of NiOOH. A part of NiOOH transformed into $Ni(OH)_2$ by capturing an electron from glucose. The generated $Ni(OH)_2$ can be oxidized to NiOOH again, which leads to the increase in the oxidation peak current and shift in the oxidation peak potential. This process can be described by reaction equations

(1) to (3). Another part of NiOOH obtains an electron from the electrode to be reduced into $Ni(OH)_2$, which can be described by reaction equation (4).

$Ni(OH)_2 + OH^- \rightarrow NiOOH + H_2O + e^-$ (1)

$NiOOH + glucose \rightarrow Ni(OH)_2 + glucolactone$ (2)

$Ni(OH)_2 + OH^- \rightarrow NiOOH + H_2O + e^-$ (3)

$NiOOH + H_2O + e^- \rightarrow Ni(OH)_2 + OH^-$ (4)

3. 3. 2 Optimal potential range for the amperometric detection of glucose

As shown in Fig.4, when the potential is higher than 0.45 V, the ordinate value of the CV curves rises linearly along with the increase in the glucose concentration. The sensitivity at different potentials is almost the same, indicating that a potential higher than 0.45 V can be applied for the amperometric detection of glucose. However, the oxidation peaks simultaneously shift to a more positive potential with the increase in glucose concentration, which results in a decrease of the oxidation peak current at 0.45 V. Thus, a very low potential results in a small linear detection range. In contrast, if the applied potential is too positive, the noise amplitude is very large that the test limit is seriously affected. Interfering organics may also be directly electro-oxidized at a very positive potential. We found that 0.48 V to 0.55V is the optimal potential range for the amperometric detection of glucose using the as-prepared $Ni(OH)_2$ nanosheets/Ni electrode. In this experiment, we selected 0.51 V as the potential in testing the steady state current response.

3. 3. 3 Amperometric detection of glucose

Fig. 5a shows the well-defined amperometric response of the as-prepared $Ni(OH)_2$ nanosheets/Ni electrode to glucose at the concentration range of 2 μM to 40 μM with a response time of less than 2 s. From the inset curve in Fig. 5a, 0.1 μM glucose clearly cannot be detected. However, when 1 μM, 2 μM, and 3 μM glucose were added in the condition, well-defined amperometric responses were observed, which indicates that the detection limit of the as-prepared $Ni(OH)_2$ nanosheets/Ni electrode is at least 1 μM at a signal-to-noise ratio of 3. The amperometric detection of high concentration glucose was also performed, the result of which was shown in Fig.5b. Two corresponding calibration curves were also obtained as shown in Fig.5c. Curve A shows the relationship between the amperometric response and glucose concentration at the range of 2 μM to 40 μM, with a sensitivity value of 1133 $\mu AmM^{-1}cm^{-2}$. Curve B shows the relationship between the amperometric response and glucose concentration at the range of 0.1 mM to 2.5 mM, with a sensitivity value of 1097 $\mu AmM^{-1}cm^{-2}$. The sensitivity, detection limit, linear range, and response time of the as-prepared $Ni(OH)_2$ nanosheets/Ni electrode were compared with previously reported typical non-enzymatic and enzymatic methods for glucose determination, which are listed in Table 1 [16,25–31].

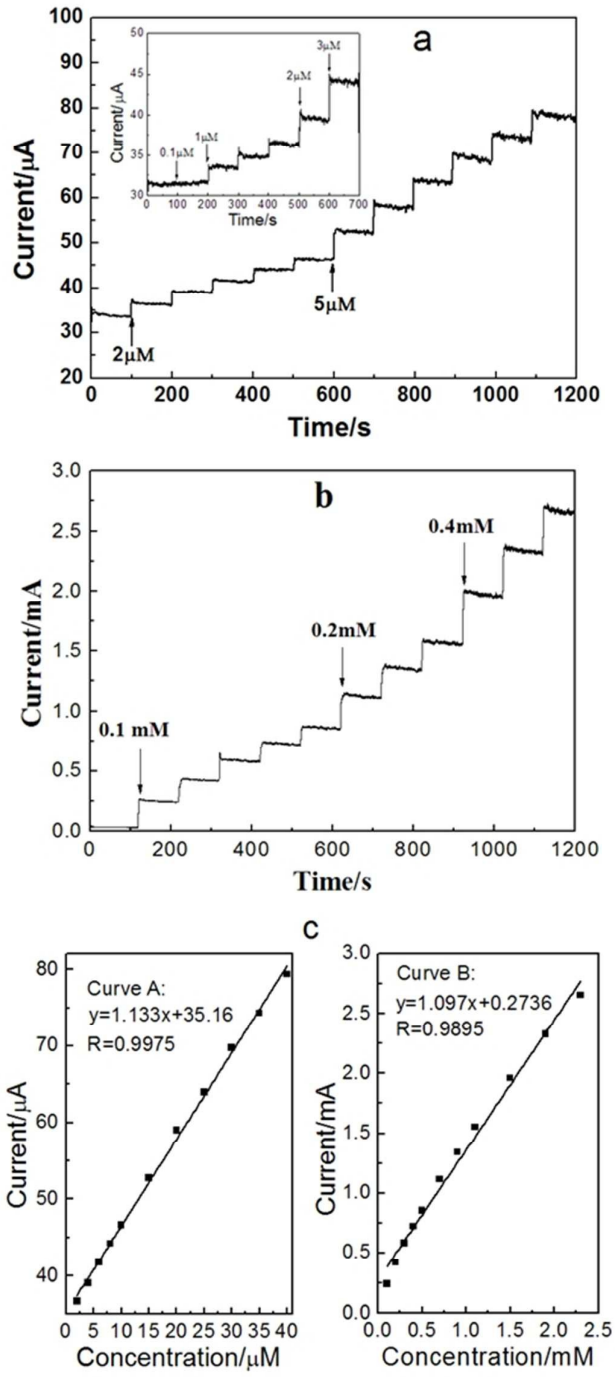

Fig. 5 (a) Amperometric responses of the $Ni(OH)_2$ nanosheets /Ni electrode toward 2 μM and 5 μM glucose concentration in 0.2 M sodium hydroxide solution at 0.51 V. (In-set) Detection limit of the $Ni(OH)_2$/Ni electrode. (b) The amperometric responses of the $Ni(OH)_2$ nanosheets/Ni electrode toward 0.1 mM, 0.2 mM, and 0.4 mM glucose concentration in 0.2 M sodium hydroxide solution at 0.51 V. (c) The corresponding calibration curves of $Ni(OH)_2$ nanosheets/Ni electrode for the determination of glucose (curve A: 2–40 μM; curve B: 0.1–2.5 mM).

Journal Name

ARTICLE

Table 1 Performances of the different glucose sensors

Electrode	Sensitivity ($\mu AmM^{-1}cm^{-2}$)	Detection limit	Response time	Reference
$Ni(OH)_2$/Ni	1130 (2-40 μM) 1097 (0.1-2.5 mM)	1 μM	< 2 s	This work
$Ni(OH)_2$/graphene	328	0.6 μM	2 s	[16]
NiO/CPEs	55.9	0.16 μM	< 5 s	[25]
Ni/MWNTs	45.3	Not given	Not given	[26]
Au micropillar	13.2	60 μM	Not given	[27]
GOx-SWNT-PVI-Os/SPE	32	0.07 μM	< 5 s	[28]
GC/CNT/HRP-GOx/PTBO	113	Not given	Not given	[29]
AuNP-SAMs-PNT/HRP-GOx	0.3	Not given	Not given	[30]
Pt/Au/C	4.7	2 μM	Not given	[31]
A/NiONFs-GO/GCE	1100	0.77 μM	< 5 s	[32]

Our $Ni(OH)_2$ nanosheets/Ni electrode clearly exhibited much higher sensitivity, comparable linear range, lower detection limit, and shorter response time compared with the previously reported glucose sensors using NiO/CILE (NiO-modified carbon paste electrode), Ni/multi-walled carbon nanotubes, $Ni(OH)_2$ and graphene nanoparticles modified glassy carbon electrode, graphene oxide, NiO nanofibers, and Nafion-modified glassy carbon electrode.

3.4 Effect of interferences on glucose oxidation

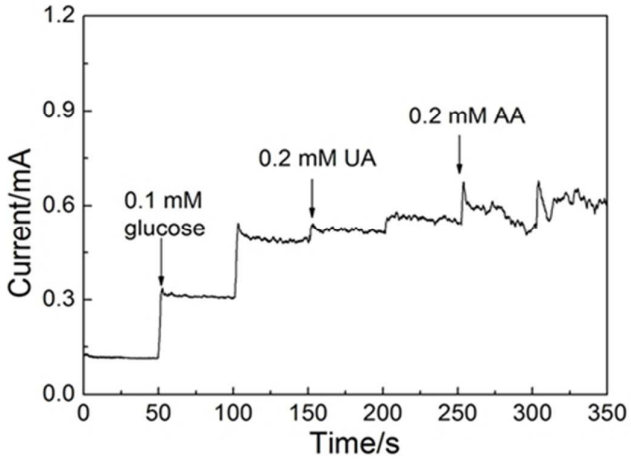

Fig. 6 Amperometric response of 0.1 mM glucose, 0.2 mM AA and 0.2 mM UA additions to the $Ni(OH)_2$ nanosheets/Ni electrode in 0.2 M NaOH.

The interference effect of 0.2 mM AA and 0.2 mM UA on the amperometric response of 0.1 mM glucose was studied in 0.2 M NaOH solution at the potential of 0.51 V to evaluate the selectivity of the as-prepared $Ni(OH)_2$ nanosheets /Ni electrode. As shown in Fig.6, the current response of 0.2 mM UA is much lower than 0.1 mM glucose, but 0.2 mM AA generates a comparative current compared with 0.1 mM glucose. The normal concentration of glucose is approximately 3 mM to 8 mM, which is much higher than the concentrations of AA (0.10 mM) and UA (0.10 mM) in the blood [26]. Thus, the two interfering species are nearly neglectable compared with that of glucose by the $Ni(OH)_2$ nanosheets/Ni electrode. All the results demonstrate that the selectivity of the sensor for glucose detection was satisfactory.

3.5 Stability and reproducibility test

The electrochemical stability of the as-prepared $Ni(OH)_2$ nanosheets/Ni electrode was tested by CV in 0.2 M sodium hydroxide solution for 100 times at a scan rate of 50 mVs-1. The oxidation peak current increased by 25%, and each scan contributed an average increment of 0.25%. However, the stability clearly improved when 0.2 mM glucose was added to the NaOH solution. The oxidation peak current only increased by 5% after 100 continuous scans. Each scan contributed an average increment of 0.05%, indicating that the $Ni(OH)_2$ nanosheets/Ni electrode was very stable. The as-prepared $Ni(OH)_2$ nanosheets/Ni electrodes were kept in sealed plastic sample bag for 50 days and then immersed into 0.2 M sodium hydroxide solution for 30 minutes before using. Both CV and constant potential amperometry technique were used to retest their performance. The oxidation peak current only dropped 8% in the same test condition. These results demonstrate that the as-prepared $Ni(OH)_2$ nanosheets/Ni

electrode has good stability. The reproducibility of as-prepared $Ni(OH)_2$ nanosheets/Ni electrode was estimated for the response at different electrodes. The response changed with a relative standard derivation of 6.7% for 10 electrodes, implying good repeatability.

Conclusions

In this study, we successfully prepared a non-enzymatic glucose sensor based on an as-prepared $Ni(OH)_2$ nanosheets/Ni electrode using a simple one-step synthetic process called the direct precipitation method. This synthetic method is simple and timesaving. All the raw materials are cheap and easy to obtain. The electrode and resulting materials were characterized by SEM, XRD, CV, and the constant potential amperometry technique. The sensitivity of the glucose sensor is as high as 1130 $\mu AmM^{-1}cm^{-2}$, whereas the detection limit is lower than 1 μM. The stability and reproducibility of this sensor are excellent. Thus, the developed tool is a promising non-enzymatic glucose sensor that can be widely used.

Acknowledgements

This research work was supported by the National Science Fund of P.R. China (NSFC Nos. 61374218).

References

1 X. Wu, M. Choi and D. Xiao, *Analyst,* 2000, **125,** 157-162.
2 E. Crouch, D. Cowell, S. Hoskins, R. Pittson and J. Hart, *Biosens. Bioelectron,* 2005, **21,** 712-718.
3 Y. Zhang, L. Su, D. Manuzzi, H. Espinosa de los Monteros, W. Jia, D. Huo and Y. Lei, *Biosens. Bioelectron*, 2012, **31,** 426-432.
4 L. Clark and C. Lyon, *Annals of the New York Academy of Sciences*, 2006, **102,** 29-45.
5 Z. Zhu, G. Luis, A. Flewitt, H. Xie, F. Moussy and W. Milne, *Sensors*, 2012, **12**, 5996-6022.
6 S. Li, J. Chou and T. Sun, *Sensor Letters*, 2011, **9,** 143-146 .
7 Q. Wang, P. Subramanian, M. Li, W. Yeap, K.Haenen, Y. Coffinier, R. Boukherroub and S. Szunerits, *Electrochem. Commun.*, 2013, **34,** 286-290.
8 C. Ko, J. Huang, S. Raina and W. Kang, *Analyst,* 2013, **138**, 3201-3208.
9 J. Luo, S. Jiang, H. Zhang, J. Jiang and X. Liu, *Anal. Chim. Acta*, 2012, **709**, 47-53.
10 S. Park, H. Boo and T. Chung, *Anal. Chim. Acta,* 2006, **556**, 46-57.
11 E. Skou, *Electrochimica Acta.*, 1977, **22,** 313-318.
12 I. Yeo and D. Johnson, *J. Electroanal. Chem,* 2000, **484**,157-163.
13 T. Satheesh Babu and T. Ramachandran, *Electrochimica Acta.*, 2010, **55**, 1612-1618.
14 Q. Yi, W. Huang, W. Yu, L. Li and X. Liu, *Electroanalysis*, 2008, **20,** 2016-2022.
15 L. Lu, L. Zhang, F. Qu, H. Lu, X. Zhang, Z. Wu, S. Huan, Q. Wang, G. Shen and R. Yu, *Biosens. Bioelectron.*, 2009, **25,** 218-223.
16 Y. Mu, D. Ji, Y. He, Y. Miao and H. Wu, *Biosens. Bioelectron.*, 2011, **26**, 2948-2952.
17 C. Wang, L. Yin, L. Zhang and R. Gao, J. Phys. Chem. C, 2010, 114, 4408–4413.
18 K. Toghill, L. Xiao, M. Phillips, R. Compton, *Sens. Actuators B,* 2010, **147,** 642–652.
19 W. Lu, X. Qin, A. Asiri, A. Al-Youbi, X. Sun, *Analyst,* 2013, **138,** 417–420.
20 C. Guo, Y. Wang, Y. Zhao, C. Xu, *Anal. Methods,* 2013, **5,** 1644–1647.
21 C. Kung, Y. Cheng, K. Ho, *Sens. Actuators B,* 2014, **204,** 159–166
22 Z. You, K. Shen, Z. Wu, X. Wang and X. Kong, *Appl. Surf. Sci.* 2012, **258**, 8117-8123.
23 Y. Li, J. Yao, Y. Zhu, Z. Zou and H. Wang, *J. Power Sources,* 2012, **203,** 177-183.
24 A. Sun, J. Zheng and Q. Sheng, *Electrochimica Acta.* 2012, **65**, 64-69
25 N. Qiao and J. Zheng, *Microchim Acta*, 2012, **177,** 103-109.
26 X. Zhang, G. Wang and Y. Huang, *The Institution of Engineering and Technology*, 2012, **7,** 168-170.
27 R. Prehn, M.C.-Puig and F.X. Muñoz, J. *The Electrochemical Society,* 2012, **159**, 134-139.
28 Q. Gao, Y. Guo, W. Zhang, H. Qi and C. Zhang, *Sens. Actuators B,* 2011, **153,** 219-225.
29 W. Wang, F. Wang, Y. Yao, S. Hu and K. Shiu, *Electrochim. Acta,* 2010, **55,** 7055-7060.
30 B.W. Park, R. Zheng, K.A. Ko, B.D. Cameron, D.Y. Yoon and D.s. Kim, *Biosens. Bioelectron.*, 2012, **38 ,** 295-301.
31 B. Singh, F. Laffir, T. Mccormac and E. Dempsey, *Sens. Actuators B,* 2010, **150,** 80-92.
32 Y. Zhang, Y. Wang, J. Jia and J. Wang, *Sens. Actuators B,* 2012, **171,** 580-587.